A two-sublattice model for light-induced hysteresis in spin-crossover solids: symmetry breaking and kinetic effects

2000 J. Phys.: Condens. Matter 12 9395

(http://iopscience.iop.org/0953-8984/12/45/303)

J. Phys.: Condens. Matter **12** (2000) 9395–9406. Printed in the UK PII: S0953-8984(00)12413-0

A two-sublattice model for light-induced hysteresis in spin-crossover solids: symmetry breaking and kinetic effects

Christophe Parreira†‡, Cristian Enachescu†§, Jorge Linarès†‖, Kamel Boukheddaden† and François Varret†

† Laboratoire de Magnétisme et d'Optique, CNRS-UMR 8634, Université de Versailles St Quentin en Yvelines, F78035 Versailles Cédex, France
‡ Université de Cergy-Pontoise, Cergy-Pontoise, France
§ 'Alexandru Ioan Cuza' University, Faculty of Physics, Iasi, 6600, Romania

Received 7 March 2000, in final form 31 July 2000

Abstract. The recently developed macroscopic model of light-induced equilibrium of spin-crossover solids is extended to the case of two equivalent sublattices coupled 'antiferromagnetically'. To do this, we use an Ising-like model involving two coupling parameters of opposite signs for the intra- and inter-sublattice interactions, previously introduced to describe the two-step static spin transition, and we have adapted the macroscopic master equation describing the time evolution of the system accordingly.

We mostly report on the quasi-static solutions of the system, under constant light irradiation and for slow temperature variations. Light-induced thermal hysteresis loops are obtained and have typical two-step shapes for suitable sets of parameter values. The model predicts, in analogy with the static transition, a possible light-induced symmetry breaking between the structurally equivalent sublattices. Kinetic effects are briefly described.

1. Introduction

Cooperative effects constitute the basic mechanism for the spin-crossover transition (see e.g. [1, 2]). They induce instability in the thermodynamic competition between the two states of the spin-crossover molecules: high spin (HS) and low spin (LS). Interactions tending to favour the pair states made of identical spin states (HS–HS or LS–LS) are usually referred to as 'cooperative' or 'ferromagnetic-like', while those tending to favour the pair states made of different spin states (HS–LS or LS–HS) are usually referred to as 'anti-cooperative' or 'antiferromagnetic-like'.

A further instability, also of cooperative origin, has been recently discovered [3, 4] and analysed in the mean-field approach [4, 5] describing the properties of cooperative photoexcitable molecular solids under permanent photoexcitation. It is worth noting that the mean-field approach is well suited to the light-induced effects, since the random character of the photoexcitation process hinders the onset of short-range correlations [6]. This light-induced instability was introduced for the single-lattice case. We present here the extension of the model to the case of a solid made of two equivalent sublattices.

Indeed, for some compounds the spin transition occurs in two steps. These compounds are made of either bi-iron [7–9] or mono-iron [10–12] molecular units. In all cases the two-step transition was modelled by introducing an 'antiferromagnetic-like' coupling, either between

‖ Author to whom any correspondence should be addressed.

0953-8984/00/459395+12$30.00

iron sites in di-iron molecular units [7, 8] or between sublattices [13, 14], or merely as a short-range interaction [15]. All models provide a 'plateau' in the middle of the conversion curve for the high-spin fraction, $n_{hs}(T)$, and the low-spin fraction, $n_{ls}(T)$, because the 'antiferromagnetic-like' interaction stabilizes an intermediate HS–LS state. When both kinds of interaction are strong, the system may exhibit thermal hysteresis with double loops.

We deal here with the two-sublattice approach, already treated analytically in the mean-field approach. The static model [13] predicts a possible symmetry breaking in a finite-temperature range associated with the 'plateau' of the conversion curve. The two sublattices, structurally equivalent far from the transition, i.e. equivalent with respect to their energy gaps, degeneracies, and interactions, become inequivalent on approaching the transition from either side. Of course, the direct observation of such a symmetry breaking by structural methods is a challenge which has not been met so far. The only study dealing with the structure of the two-step transition complex [Fe^{II}(5-NO_2-sal-N(1, 4, 7, 10))] [12] reports inequivalent sublattices at all temperatures.

We present here a novel extension of the mean-field model of light-induced instability [4,5], adapted to the case of the two-sublattice system. The features expected intuitively are two-step light-induced hysteresis loops and light-induced symmetry breakings. These features, as will be shown below, are effectively produced by the model.

2. The light-induced equilibrium (after [4])

The light-induced equilibrium in the system $[Fe^{II}_x Co_{1-x}(btr)_2(NCS)_2]\cdot H_2O$ was analysed [4], as follows: at low temperature the ground state is LS which has a strong optical absorption in the visible. On irradiating into a LS-state absorption band the molecules are switched to the metastable HS state by the LIESST (light-induced excited spin-state trapping) effect [2, 16]. After photoexcitation, the photoinduced metastable state (HS) relaxes to the ground state (LS). The relaxation curve shape is sigmoidal, which is a signature of a cooperative relaxation process [17–20]: the energy barrier of the metastable state progressively decreases while relaxation proceeds, leading to a 'self-accelerated' kinetics. Experimental data (above the tunnelling process temperature range) are consistent with a thermal activation process involving an energy barrier $E_a(n_{hs})$ depending linearly on the high-spin fraction n_{hs}. Accordingly, the relaxation of the system is written as

$$\left(\frac{\mathrm{d}n_{hs}}{\mathrm{d}t}\right)_{rel} = -n_{hs}k_{HL}(T, n_{hs}) = -n_{hs}k_\infty \exp\left(-\frac{E_a(n_{hs})}{k_B T}\right) \tag{1}$$

where

$$E_a(n_{hs}) = E_a(0) + a n_{hs} \tag{2}$$

with E_a the activation energy of the molecule for the HS $\rightarrow$ LS relaxation and k_∞ the high-temperature limit of the relaxation rate. The 'self-accelerator parameter' a, of cooperative origin, is obviously related to the self-acceleration factor α introduced by Hauser *et al* [17] in the following form:

$$k_{HL}(T, n_{hs}) = k_{HL}(T, 0)\exp(-\alpha n_{hs}) \tag{3}$$

where

$$a = \alpha k_B T. \tag{4}$$

It is worth noting that a is by definition temperature independent, while α, which is the measured quantity, is observed to be temperature dependent. The above relation between a and α is of course restricted to the thermally activated relaxation regime. It has been verified

by all investigations made so far [2, 4, 17–20], above the temperature range for which the tunnelling regime is prominent.

The self-acceleration parameter a is expected to be proportional to the mean-field interaction parameter on the basis of both experimental (see above) and theoretical results [18, 21].

Under permanent irradiation (of appropriate wavelength), photoexcitation occurs, which is responsible for the LIESST effect. The photoexcitation term is proportional to the number of molecules in the LS state, i.e. available for the photoexcitation process. A constant, single-site excitation rate, such that one absorbed photon drives exactly one spin-crossover unit into the excited state, is assumed. The excitation term can be expressed as

$$\left(\frac{\mathrm{d}n_{hs}}{\mathrm{d}t}\right)_{exc} = (1 - n_{hs})I_0\sigma \tag{5}$$

where I_0 is the intensity of the irradiation and σ is a constant accounting for the number and cross section of the spin-crossover molecules†. The master equation which governs the evolution of the system accounts for both processes, and is written here as

$$\frac{\mathrm{d}n_{hs}}{\mathrm{d}t} = (1 - n_{hs})I_0\sigma - n_{hs}k_\infty \exp\left(-\frac{E_a(0)}{k_BT}\right)\exp(-\alpha n_{hs}). \tag{6}$$

In this equation, the reverse relaxation, i.e. LS $\rightarrow$ HS, has not been accounted for because at the temperatures considered the corresponding probability is very weak.

The steady state of the system is such that $\mathrm{d}n_{hs}/\mathrm{d}t = 0$. Thus equation (6) can be expressed as

$$(1 - n_{hs})I_0\sigma = n_{hs}k_\infty \exp\left(-\frac{E_a(0)}{k_BT}\right)\exp(-\alpha n_{hs}). \tag{7}$$

This is the state equation of the photostationary states of the system. A useful concept is that of the 'photoinduced equilibrium temperature', which can be expressed as

$$k_BT^*_{equil} = \frac{E_a(1/2)}{\ln(k_\infty/[I_0\sigma])}. \tag{8}$$

The non-linear character of equation (7), due to the self-accelerated relaxation, is responsible for the occurrence of instability, for $\alpha(T^*_{equil}) > 4$ [4, 5]. We show in figure 1 the S-shaped curve associated with the light-induced instability of the steady states of the one-sublattice system. The thermal hysteresis associated with this S-shaped curve has been called light-induced thermal hysteresis (LITH) [3].

3. The two-sublattice extension

Extension of equations (6), (7) to the two-sublattice case requires a convenient expression for the cooperative terms. It is worth recalling that the self-acceleration parameter a is associated with the interaction strength. The Ising-like mean-field model used in [13, 14] is perfectly suited to describe this effect, since it provides an energy gap between the two states which varies linearly with the high-spin fraction:

$$\Delta(n_{hs}) = \Delta(0) - 4Jn_{hs}. \tag{9}$$

This is consistent with a barrier energy that is linearly dependent on the high-spin fraction, as introduced in [17], and finally provides a linear relationship between J and a. Indeed, the first

† It is worth noting that the assumption of a linear, single-site character for the photoexcitation process has recently been challenged by the emergence of two counter-examples: the complex $[Fe^{II}(bt)(NCS)_2]_2(bpym)$ made of bi-iron molecular units [22] and an experiment using an extremely intense laser beam [23], giving evidence for the so-called domino effect.

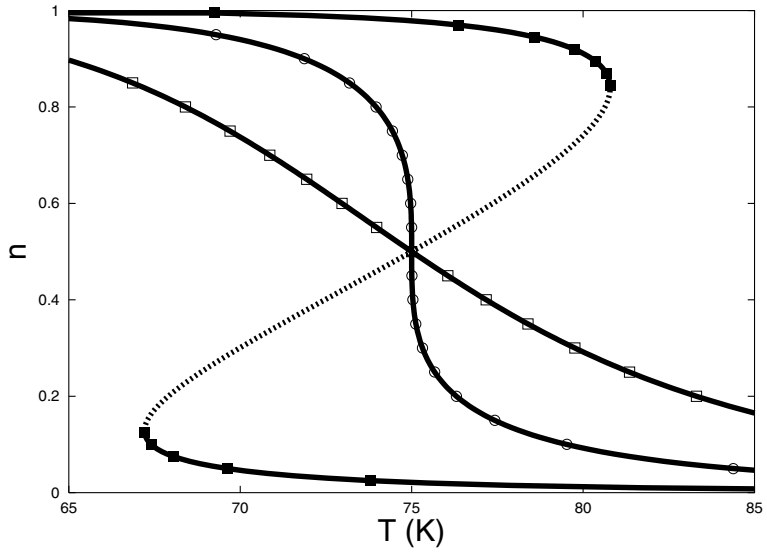

Figure 1. Computed light-induced thermal hysteresis for a one-sublattice system (adapted from [4]). The unstable states have been reported as a dotted line. The parameter values are as follows: $T^*_{equil} = 75$ K, $I_0\sigma/k_\infty = 5.58 \times 10^{-6}$, $E_a(1/2) = 729$ K, $\alpha T = 50$ (open squares), 300 (open circles), 600 K (full squares). Above the threshold value, hysteresis occurs.

direct experimental evidence for such a linear relationship was recently obtained from a study of the diluted series $[Fe^{II}_xCo_{1-x}(btr)_2(NCS)_2]\cdot H_2O$ [24]. Thus, the self-acceleration parameter can be expressed as

$$a = \frac{\mathrm{d}E_a(n_{hs})}{\mathrm{d}n_{hs}} = \frac{\mathrm{d}E_a(n_{hs})}{\mathrm{d}\Delta(n_{hs})}\frac{\mathrm{d}\Delta(n_{hs})}{\mathrm{d}n_{hs}} = -4J\frac{\mathrm{d}E_a(n_{hs})}{\mathrm{d}\Delta(n_{hs})} \tag{10}$$

and the self-acceleration factor as

$$\alpha = \frac{a}{k_BT} = -\frac{4J}{k_BT}\frac{\mathrm{d}E_a(n_{hs})}{\mathrm{d}\Delta(n_{hs})} = \gamma\frac{J}{T} \tag{11}$$

where γ is a proportionality factor specific to the nature of the spin-crossover unit, irrespective of the lattice site or sublattice to which it belongs.

For the system made of two structurally equivalent sublattices [13], the relevant interaction parameters are

- $J = J_{intra} > 0$, intra-sublattice interaction;
- $J_{AB} = J_{inter} < 0$, inter-sublattice interaction.

A negative sign for J_{AB} is needed for the two-step transition [13]. It induces the relative stabilization of the HS–LS state of the system (one sublattice HS, the other LS), which becomes the stable state of the system at the plateau of the conversion curve $n_{hs}(T)$. Accordingly, we define the following two factors:

- a self-acceleration factor, $\alpha = \gamma J/T > 0$, associated with the intra-sublattice (positive) interaction;
- a self-deceleration factor, $\beta = \gamma J_{AB}/T < 0$, associated with the inter-sublattice (negative) interaction.

For each of the sublattices, these two effects merely add up within the expression of the barrier energy, i.e. in the argument of the exponential factor of the relaxation rate. High-spin

fractions also have to be defined for the two sublattices, $n_{hs}^{(A)}$, $n_{hs}^{(B)}$, and obviously their roles in the self-acceleration and deceleration effects are interchanged for the two sublattices. On the other hand, the photoexcitation effect is assumed to occur at a constant single-site rate, irrespective of the sublattice. Following these simple mean-field assumptions, the master equation is written as the following set of coupled differential equations:

$$\begin{cases} \dfrac{\mathrm{d}n_{hs}^{(A)}}{\mathrm{d}t} = (1 - n_{hs}^{(A)})I_0\sigma - n_{hs}^{(A)}k_\infty \exp\left(-\dfrac{E_a(0)}{k_BT}\right)\exp(-\alpha n_{hs}^{(A)} - \beta n_{hs}^{(B)}) \\ \dfrac{\mathrm{d}n_{hs}^{(B)}}{\mathrm{d}t} = (1 - n_{hs}^{(B)})I_0\sigma - n_{hs}^{(B)}k_\infty \exp\left(-\dfrac{E_a(0)}{k_BT}\right)\exp(-\alpha n_{hs}^{(B)} - \beta n_{hs}^{(A)}). \end{cases} \tag{12}$$

With simpler notation, detailed below, the coupled equations (12) appear as

$$\begin{cases} \dot{x} = k_\infty\left[p(1-x) - xE\exp(-\alpha x - \beta y)\right] \\ \dot{y} = k_\infty\left[p(1-y) - yE\exp(-\alpha y - \beta x)\right] \end{cases} \tag{13}$$

with: $x = n_{hs}^{(A)}$, $y = n_{hs}^{(B)}$, $\dot{x} = \mathrm{d}x/\mathrm{d}t$, $\dot{y} = \mathrm{d}y/\mathrm{d}t$, $p = I_0\sigma/k_\infty$, $E = \exp(-E_a(0)/kT)$.

Formally, the coupled equations (13) are those of the Eulerian description of a compressible and rotational fluid.

The photostationary states of the two-sublattice model are such that the velocity components $\dot{x}$, $\dot{y}$ are null. The coupled equations for the quasi-static (photostationary) solutions, i.e. the state equations of the light-induced states, are

$$\begin{cases} p(1-x) = xE\exp(-\alpha x - \beta y) \\ p(1-y) = yE\exp(-\alpha y - \beta x). \end{cases} \tag{14}$$

4. Results and discussion

4.1. The photostationary states

The resolution of the coupled set of equations (14), i.e. the search for x, y for given values of the independent parameters p, E, α, β, is usually performed numerically. It may be worth considering that these parameters derive from the independent physical quantities T, $E_a(0)$, γJ, γJ_{AB}, $I_0\sigma/k_\infty$, the first four of which are energetic quantities; the last one is dimensionless. For the resolution of the master equation (13), time t is a further variable, and $I_0\sigma$, k_∞ are independent parameters with the dimension of inverse time.

The maximum number of solutions of equations (14) may be determined by a graphical investigation in the (x, y) plane. Equations (14) define two curves whose intercepts are required. Interestingly, this method, elsewhere considered as the 'nullcline method' (see e.g. [25]), is suitable for investigating the hydrodynamic problem associated with the multidimensional equation (13).

The function $y(x)$ associated with the *first* equation (14) can be expressed explicitly as

$$y = \frac{1}{\beta}\left[\ln\frac{x}{1-x} - \alpha x + \ln\frac{E}{p}\right] \tag{15}$$

$$y' = \frac{\mathrm{d}y}{\mathrm{d}x} = \frac{1}{\beta}\left[\frac{1}{x(1-x)} - \alpha\right] \tag{16}$$

$$y'' = \frac{1}{\beta}\left[\frac{1-2x}{x^2(1-x)^2}\right]. \tag{17}$$

The functions $y(x)$, $y'(x)$, $y''(x)$ are defined and continuous for $x \in]0, 1[$. The values of E and p are necessarily positive, and β has been taken negative in the model. Then $y(x)$ has asymptotic branches $y \to \infty$ for $x \to 0$ and $y \to -\infty$ for $x \to 1$. For $\alpha = 0$, $y(x)$ is a monotonic decreasing function which does not provide hysteresis. It possesses an inflection point at $x = 1/2$, with a slope which becomes positive for $\alpha > 4$. The resulting instability, quoted in [4], is clearly associated with the S-shaped character of the curve. The branch with positive slope corresponds to an unstable state of sublattice A (for a frozen sublattice B, i.e. at fixed y).

The function $x(y)$ associated with the *second* equation (14) has identical properties (interchanging x, y). Typical curves are reported in figure 2 and clearly show that the problem may have up to nine solutions, with one or three symmetrical solutions ($x = y$) and eventually two or three symmetric pairs of asymmetric solutions ($x \neq y$), according to the parameter values.

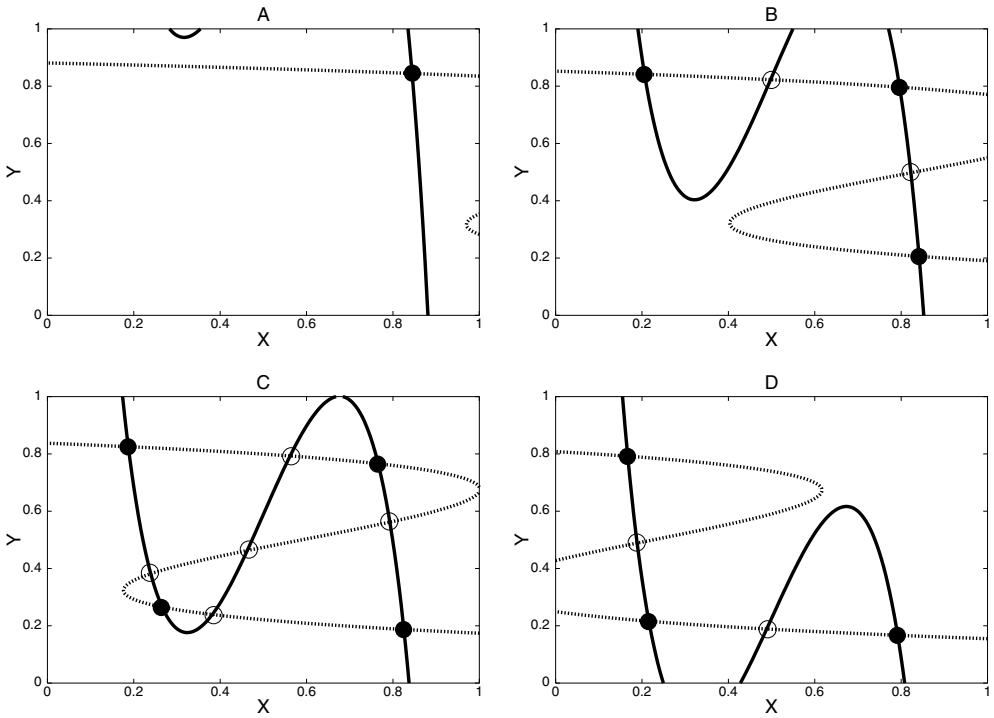

Figure 2. Graphical determination of the steady states, using the curves $y(x)$, $x(y)$, associated with equations (14) (full line and dashed line for the first and second equation, respectively). The temperature values are (a) far below the LITH loop, (b) in the first part of the LITH loop, (c) at the light-induced equilibrium temperature, (d) at the bifurcation point of the heating branch ($B^{\uparrow}$). The same notation is also used in the next figure. The other parameter values are as follows: $p = 5.58 \times 10^{-6}$, $E_a(1/2) = 729$ K, $\alpha T = 275$ K, $\beta T = -10$ K. Full and open symbols circles indicate stable and unstable solutions, respectively.

The problem now is that of determining the stability of these solutions. It may be resolved by the numerical method of flow diagrams in the (x, y) plane. The method consists in calculating, using the master equations, a large number of trajectories in the parameter space $(x(t), y(t))$. Here we bypass this onerous task using the nullclines method, i.e. taking advantage of the direct knowledge of the sign of the velocity components $\dot{x}$, $\dot{y}$, given by equations (13).

This can be followed in figure 2. Indeed, since $\beta < 0$, $\dot{x}(x, y)$ is a decreasing function of y, i.e. it is positive below the curve $y(x)$ and negative above this curve. Similarly, $\dot{y}(x, y)$ is a decreasing function of x, i.e. $\dot{y}$ is positive on the left-hand side of the curve $x(y)$ and negative on the right-hand side of this curve. The knowledge of these signs enables us to determine whether the solutions associated with the intercepts of the B curves, as shown in figure 3, have stable or unstable character. In this way, we have obtained the simple rule that any reversed branch of the S-shaped curves (or combination thereof) in the (x, y) plane necessarily leads to instability. This is a simple two-dimensional extension of the usual instability criterion for the (n, T) plane.

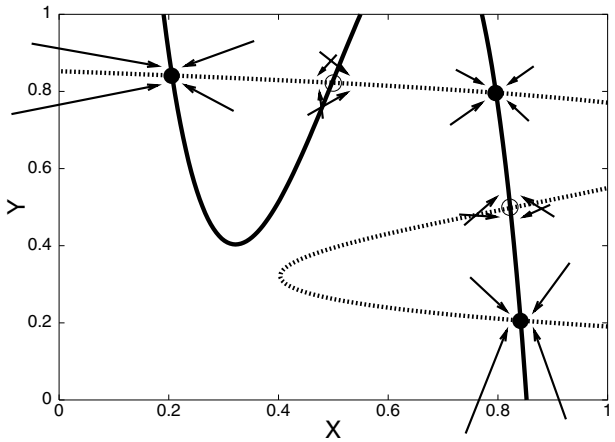

Figure 3. Investigation of the stability of the steady-state solutions, for the situation shown in figure 2(b). The signs of the velocity components have been determined as explained in the text. The resulting stability or instability of the character of the solutions is indicated by full and open circles, respectively.

4.2. The photostationary light-induced thermal hysteresis loops

In the present section we analyse the behaviour of the two-sublattice system under permanent irradiation, subjected to extremely slow temperature variations, such that the state equations of the photostationary states can be used. A typical set of n_{hs}-curves is shown in figure 4. Whether the solutions have stable or unstable character has been determined as explained in the previous section. For clarity, we have reported the average high-spin fraction of the two sublattices (figure 4(a)) and the high-spin fraction for each sublattice (figure 4(b)). The symmetrical solutions are identical to those for the one-sublattice system, shown earlier in figure 1, with the typical S-shaped thermal curve, and unstable states occur around the light-induced equilibrium temperature.

The novelty of the two-sublattice system is provided by the non-symmetric solutions which appear in a limited temperature range around the light-induced equilibrium temperature, shown in figure 4(b). According to the previous section, the solutions obtained at a given temperature for each sublattice have to be combined so as to form two or three symmetric pairs of asymmetric solutions. These are indicated in the figure. It can be seen that, on increasing temperature, the asymmetric solutions reach a collapse point ($B^{\uparrow}$), called a 'bifurcation point', on the branch of the symmetric solution. Beyond $B^{\uparrow}$ the states of the symmetric branch are unstable. By the instability criterion, the $[B^{\uparrow/\downarrow}, S_S^{\uparrow/\downarrow}]$ part of the curve is unstable. The stable asymmetric

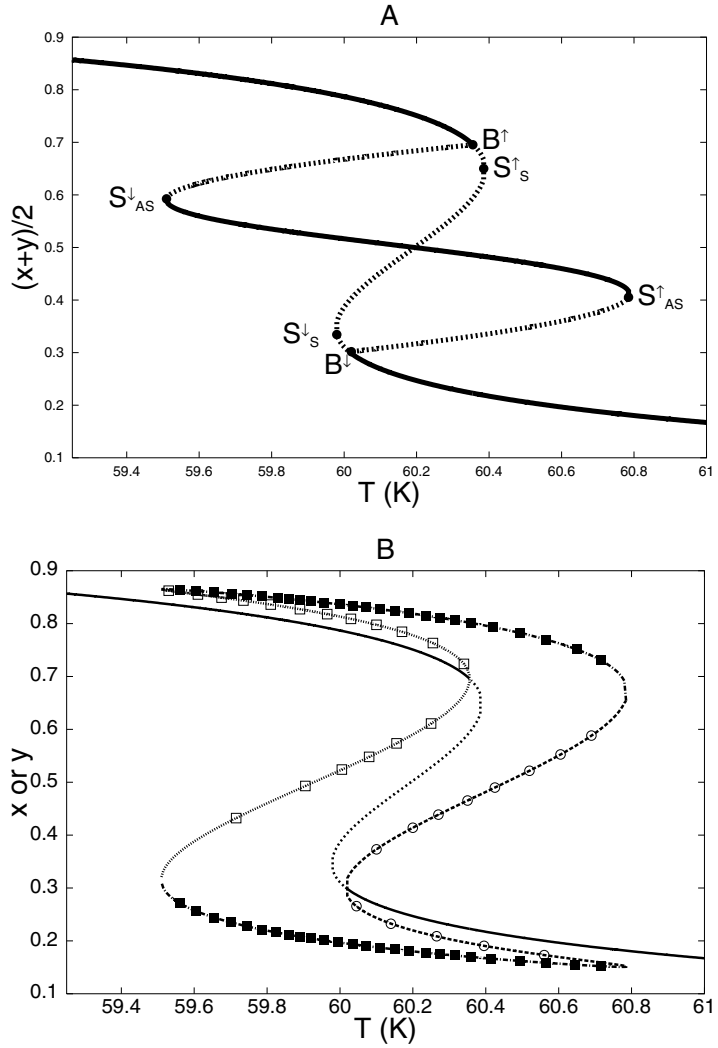

Figure 4. The set of steady-state solutions, at constant intensity, plotted as $n_{hs}(T)$ curves. The computed data are reported averaged (a) or separately (b) for the sublattices. The stable and unstable branches are shown as full and dotted lines, respectively. In (b), the asymmetric solutions are obtained as pairs of curves, associated as shown by lines of same symbols. The unstable asymmetric solutions collapse at the bifurcation points ($B^{\uparrow}$, $B^{\downarrow}$). Accordingly, the symmetric branches are no longer stable beyond these bifurcation points.

branch goes through the instability point and is limited by asymmetric spinodal points ($S^{\uparrow}_{AS}$ and $S^{\downarrow}_{AS}$). We show in the next section how the instability at the light-induced equilibrium can be 'resolved' thanks to the symmetry breaking of the system.

4.3. The occurrence of the light-induced symmetry breaking

We again consider here the quasi-static states, i.e. the solutions of the steady-state equations (14). The thermal variation of the average high-spin fraction is deduced, in principle, by following the stable states by continuity. However, at the bifurcation points, the system which

leaves a stable state 'has to choose' between two stable states. The actual pathway of the system can be determined by using the flow diagram method, in the simple analytical form used in a previous section, and the result is that the system does indeed go to the asymmetric state, i.e. follows the intermediate branch; see figure 5. It follows that the complete LITH loop splits into two parts. The middle part of the asymmetric solution branch, i.e. in the $[T_{B\downarrow}, T_{B\uparrow}]$ temperature range, is only accessible by a reversal of the temperature variation; in other words it belongs to a minor hysteresis loop.

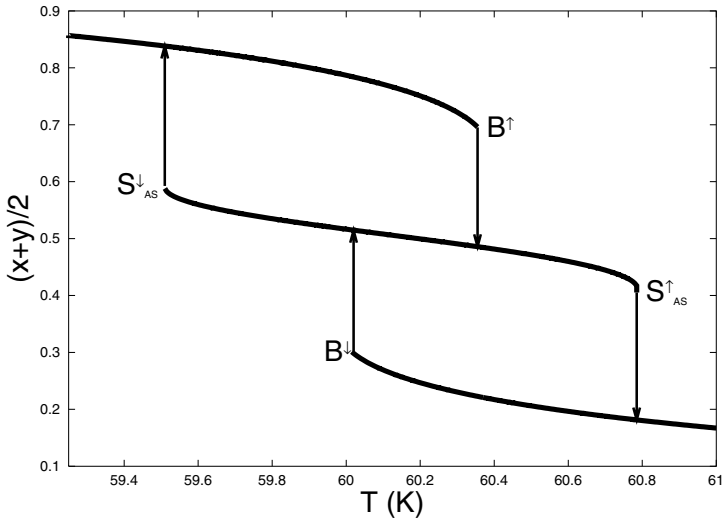

Figure 5. The pathway along the LITH loop, reported as thick lines. Beyond the bifurcation points ($B^{\uparrow}$, $B^{\downarrow}$), the spontaneous symmetry breaking may occur via vanishingly small additional asymmetries.

One may wonder how the light-induced symmetry breaking occurs. As for any disorder–order transformation, it has to be triggered by tiny perturbations, e.g. thermal fluctuations or merely by the discontinuous character of the photon flux. In the present continuous mean-field model, a small asymmetry added to any parameter involved in the master equation is sufficient to trigger the symmetry breaking.

We have computed the steady states, for several values of the inter-sublattice interaction parameter γJ_{AB}. The parameter values have been chosen so as to provide identical symmetric solutions, with $\gamma J + \gamma J_{AB} =$ constant. The data are reported in figure 6 and show that the larger γJ_{AB}, the wider the asymmetric branch, with the larger distance between the bifurcation point ($B^{\uparrow/\downarrow}$) and the spinodal point ($S_S^{\uparrow/\downarrow}$) of the symmetric branch. In the particular case of uncoupled sublattices ($J_{AB} = 0$), B and S_S coincide, so the asymmetric branch cannot be reached by usual (macroscopic) means.

4.4. The comparison to the metamagnetic transition

The comparison with magnetic systems is now briefly described. The competition between interactions of opposite signs, i.e. between ferromagnetic and antiferromagnetic ones, may lead to the 'metamagnetic' transition [26] which is the transformation from an antiferromagnetic state into a ferromagnetic state under the effect of an external magnetic field. The symmetry between the structurally equivalent sublattices is restored by the application of the field. In the Ising-like system considered here, the concept of a temperature-dependent field, due

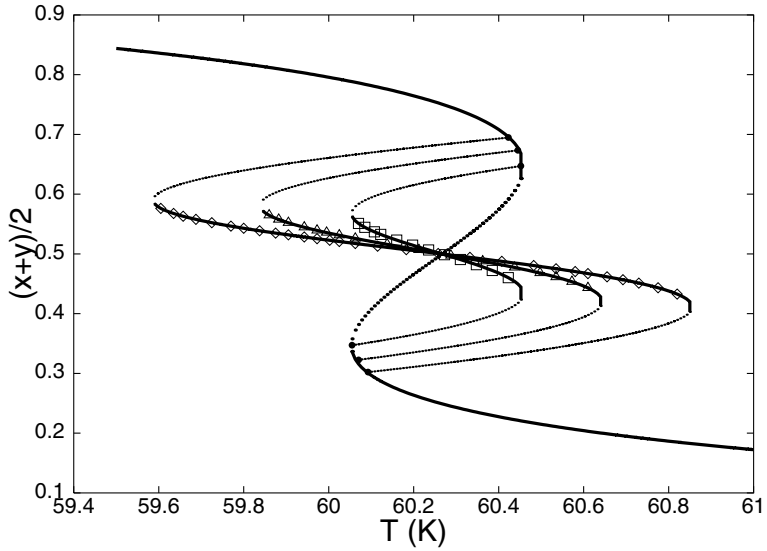

Figure 6. LITH loops, computed for different values (in K) of the coupling parameters: $(\alpha T, \beta T) = (275, 0), (280, -5), (285, -10)$. The other parameter values are those of figures 2 to 5. Unstable solutions are shown as dotted lines. The values of βT are 0 K, −5 K, and −10 K for squares, triangles, and rhombuses respectively.

to Doniach [27], is useful: the two-level system with different degeneracies ('Ising-like') is equivalent to a two-level system with equal degeneracies ('pure Ising') subjected to the temperature-dependent field:

$$\Delta(T, n_{hs}) = \Delta(0) - 4Jn_{hs} - k_B T \ln \frac{g_{hs}}{g_{ls}}. \tag{18}$$

Let us discuss first the static transition: at the equilibrium temperature, the effective field $\Delta(T_{equil}, n_{hs} = 1/2)$ vanishes, and the state of the system, mostly in the HS–LS state, is analogous to the antiferromagnetic state. When temperature is shifted on either side of T_{equil}, the effective field arises and induces the transition to the HS state (on increasing temperature) or to the LS state (on decreasing temperature). This is analogous to the metamagnetic transition, but occurs on each side of the equilibrium temperature.

The analogy holds also for the light-induced transition. The one-sublattice expression (7) for the steady state of the system should be transformed to the following form:

$$\frac{1 - n_{hs}}{n_{hs}} = \exp\left[-\frac{1}{k_B T}\left(E_a(0) + an_{hs} - k_B T \ln \frac{k_\infty}{I_0 \sigma}\right)\right] = \exp\left[-\frac{\Delta^*(T, n_{hs})}{k_B T}\right]. \tag{19}$$

Equation (19) introduces the concept of a light-induced effective field $\Delta^*(T, n_{hs})$, which is temperature dependent, and which cancels at the light-induced equilibrium temperature and includes the interaction terms. With $k_\infty \gg I_0\sigma$, the effect is analogous to that of the static effective field, given by equation (18), except for the interchange between the HS and LS states.

4.5. Kinetic effects

We now consider the effects of the finite kinetics, $\mathrm{d}T/\mathrm{d}t \neq 0$, necessarily involved in any experiment. The equations governing the evolution of the system are the set of coupled differential equations (13), which have to be solved numerically, using the Runge–Kutta

methods. We did not perform an extensive study of these kinetic effects; instead we restrict our analysis to the case of slow kinetics, to investigate small departures from the steady states investigated in the previous sections. For example, the hysteresis loops no longer have sharp edges, and the low-temperature edge is more disturbed than the high-temperature one [21]. The most interesting feature here is the symmetry breaking: since it obviously requires the introduction of a (vanishingly small) asymmetrization of the parameter values, we have slightly modified the energy gaps and thus obtained the curves reported in figure 7. At the slowest temperature sweep rate, the pathway is very close to that of the steady states, shown in figure 5; the conclusions derived from figure 5 are thus supported.

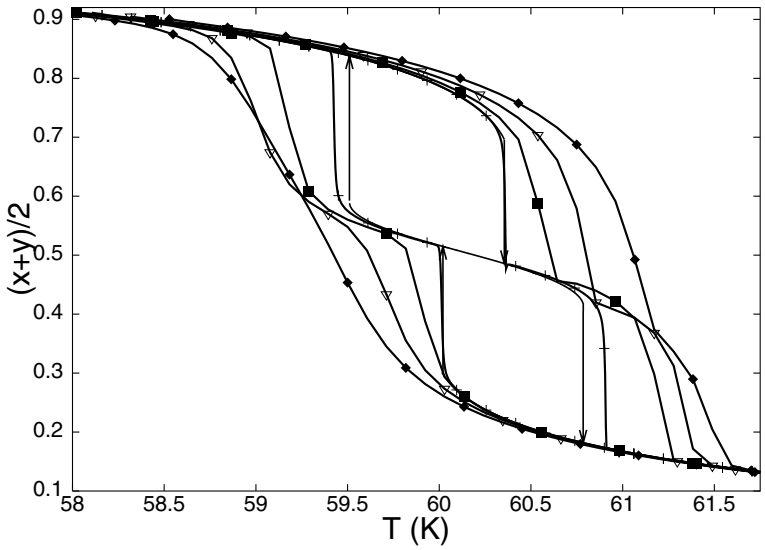

Figure 7. Kinetic effects on the LITH loop, computed for several values of the temperature sweep rate, using the set of master equations (13). The parameter values are those of figures 2 to 5, with a tiny additional asymmetry of the energy gaps. The stable quasi-static branches (steady states) are shown for comparison (vertical arrows). The temperature sweeping rates in reduced units (10^{-8} k_∞ K s^{-1}) are as follows: 0 (lines), 25 (crosses), 50 (solid squares), 125 (triangles), and 250 (rhombuses). For the rate 250, the low-temperature branch is more affected (the double step disappears) than the high-temperature branch.

It appears that the split character of the LITH disappears at high sweep rates, in the cooling mode, and is strongly reduced in the heating mode. Interestingly, similar kinetic effects are to be expected at the static transition, since the symmetry breaking requires the onset of (negative) correlations, i.e. takes time.

5. Conclusions

The phenomenological macroscopic model of light-induced effects in cooperative spin-crossover solids has been extended to the case of a two-sublattice system containing anti-cooperative inter-sublattice interactions. The calculated light-induced properties are reminiscent of the well-known static properties, with the typical double-step transition. The possible light-induced symmetry breaking of the system is a fascinating feature which should stimulate experimental work on these peculiar spin-crossover solids. Accurate structural determinations are needed before an experimental case can be properly documented.

Acknowledgments

This work was supported by the European Community: TMR (contract 'TOSS' ERB-FMRX-CT98-0199) and the Socrates programme (CE was on a Socrates grant).

References

[1] König E, Ritter G and Kulshreshtha S K 1985 *Chem. Rev.* **85** 219
[2] Gütlich P, Hauser A and Spiering H 1994 *Angew. Chem. Int. Edn Engl.* **33** 2024
[3] Letard J F, Guionneau P, Rabardel L, Howard J A K, Goeta A E, Chasseau D and Kahn O 1998 *Inorg. Chem.* **37** 4432
[4] Desaix A, Roubeau O, Jeftic J, Haasnoot J G, Boukheddaden K, Codjovi E, Linarès J, Nogués M and Varret F 1998 *Eur. Phys. J.* B **6** 183
[5] Varret F, Boukheddaden K, Jeftic J and Roubeau O 1999 *Proc. ICMM'98 (Seignosse, France); Mol. Cryst. Liq. Cryst.* **335** 561
[6] Hauser A 1997 *J. Phys. Chem. Solids* **59** 265
[7] Real J A, Bolvin H, Bousseksou A, Dworkin A, Kahn O, Varret F and Zarembowitch J 1992 *J. Am. Chem. Soc.* **114** 4650
[8] Bousseksou A, Varret F and Nasser J 1993 *J. Physique* I **3** 1463
[9] Real J A, Castro J, Bousseksou A, Verdaguer M, Burriel R, Castro M, Linarès J and Varret F 1997 *Inorg. Chem.* **36** 455
[10] Köppen H, Müller E W, Köhler C P, Spiering H, Meissner E and Gütlich P 1982 *Chem. Phys. Lett.* **91** 348
[11] Petrouleas V and Tuchagues J P 1987 *Chem. Phys. Lett.* **135** 21
[12] Boinnard D, Bousseksou A, Dworkin A, Savariault J M, Varret F and Tuchagues J P 1994 *Inorg. Chem.* **33** 271
[13] Bousseksou A, Nasser J, Linarès J, Boukheddaden K and Varret F 1992 *J. Physique* I **2** 1381
[14] Bousseksou A, Nasser J and Varret F 1995 *J. Magn. Magn. Mater.* **140** 1511
[15] Romstedt H, Hauser A, Spiering H and Gütlich P 1998 *J. Phys. Chem. Solids* **59** 1353
[16] Decurtins S, Gütlich P, Köhler C P, Spiering H and Hauser A 1984 *Chem. Phys. Lett.* **1** 139
[17] Hauser A, Gütlich P and Spiering H 1986 *Inorg. Chem.* **25** 4245
[18] Adler P, Hauser A, Vef A, Spiering H and Gütlich P 1989 *Hyperfine Interact.* **47** 343
[19] Hauser A, Jeftic J, Romstedt H, Hinek R and Spiering H 1999 *Coord. Chem. Rev.* **190–192** 471
[20] Jeftic J and Hauser A 1996 *Chem. Phys. Lett.* **248** 458
[21] Boukheddaden K, Shteto I, Hoo B and Varret F 2000 *Phys. Rev.* B submitted
[22] Létard J F, Real J A, Moliner N, Gaspar A B, Capes L and Kahn O 1999 *J. Am. Chem. Soc.* **121** 10 630
[23] Ogawa Y, Koshihara S, Koshino K, Ogawa T, Urano C and Takagi H 2000 *Phys. Rev. Lett.* **84** 3181
[24] Enachescu C, Linarès J and Varret F 2000 *J. Phys.: Condens. Matter* submitted
[25] Alligood K T, Sauer T D and York J A 1997 *CHAOS: an Introduction to Dynamical Systems* (Berlin: Springer)
[26] Jacob I S 1961 *J. Appl. Phys.* **32** 619
[27] Doniach S 1978 *J. Chem. Phys.* **68** 11